Journal of Hazardous Materials 189 (2011) 301–307

Contents lists available at ScienceDirect

Journal of Hazardous Materials

journal homepage: www.elsevier.com/locate/jhazmat

High temperature capture of CO_2 on lithium-based sorbents from rice husk ash

Ke Wang, Xin Guo*, Pengfei Zhao, Fanzi Wang, Chuguang Zheng

State Key Laboratory of Coal Combustion, Huazhong University of Science and Technology, Wuhan 430074, PR China

ARTICLE INFO

Article history:
Received 31 October 2010
Received in revised form 14 February 2011
Accepted 14 February 2011
Available online 22 February 2011

Keywords:
CO_2
Rice husk ash
Sorption/desorption
Alkali metals
Li_4SiO_4

ABSTRACT

Highly efficient Li_4SiO_4 (lithium orthosilicate)-based sorbents for CO_2 capture at high temperature, was developed using waste materials (rice husk ash). Two treated rice husk ash (RHA) samples (RHA1 and RHA2) were prepared and calcined at 800 °C in the presence of Li_2CO_3. Pure Li_4SiO_4 and RHA-based sorbents were characterized by X-ray fluorescence, X-ray diffraction, scanning electron microscopy, nitrogen adsorption, and thermogravimetry. CO_2 sorption was tested through 15 carbonation/calcination cycles in a fixed bed reactor. The metals of RHA were doped with Li_4SiO_4 resulting to inhibited growth of the particles and increased pore volume and surface area. Thermal analyses indicated a much better CO_2 absorption in Li_4SiO_4-based sorbent prepared from RHA1 (higher metal content sample) because the activation energies for the chemisorption process and diffusion process were smaller than that of pure Li_4SiO_4. RHA1-based sorbent also maintained higher capacities during the multiple cycles.

1. Introduction

At present, carbon-based fossil fuels provide ~80% of the world's energy needs [1], and causes increased level of atmospheric carbon dioxide, which is a major concern regarding climate change [2,3]. However, conversion from fossil fuels to non-fossil fuel is unlikely to occur despite increasing development of renewable (cleaner) energy sources [4] because of the long lifetime (resulting from economic considerations) of the energy supply infrastructure and other reasons. Thus, development of efficient and cost-effective means for carbon capture and (underground) storage (CCS) is urgently needed [5]. The temperature of the flue gas between the turbine and the vent are usually in the range of 352–627 °C [6]. Thus, if CO_2 is separated from flue gas at high temperature and further used as feedstock for the synthesis of fuels (e.g., CO and H_2), the efficiency and economics of the entire process of the power plant might be improved [7,8]. A critical need to study suitable sorbents for CO_2 capture at high temperature exists.

Recently, a series of lithium-based ceramics, including $Li_{2-x}Na_xZrO_3$ [9,10], Li_4SiO_4 [11], Li_4TiO_4 [12], $Li_{2+x}CuO_{2+x/2}$ [13], and Li_5AlO_4 [14], have been studied for CO_2 absorption at high temperature. Among all these ceramics, Li_4SiO_4 has received further attention because of its high sorption capacity, long-term durability, fast sorption/desorption kinetics, and good mechanical strength properties. For example, during the first few minutes, Li_4SiO_4 can absorb four or more times more CO_2 than other lithium ceramics, such as lithium metazirconate (Li_2ZrO_3) [15]. Furthermore, Li_4SiO_4 has shown excellent cyclability properties for CO_2 sorption/desorption [16]. In this case, several authors [17,18] have reported the CO_2 capture in this material through the following reaction.

$$Li_4SiO_4 + CO_2 \leftrightarrow Li_2CO_3 + Li_2SiO_3 \quad (1)$$

Li_4SiO_4 can be synthesized using different methods: the common solid-state reaction [12], precipitation method [18], impregnation suspension method [19] and sol–gel method [8,20]. The common solid-state method usually involves a solid mixture of amorphous silica (SiO_2) and a lithium compound, such as Li_2CO_3, heated in air for a long time between 700 and 1000 °C to produce lithium silicate powders. The inherent reactivity of Li_4SiO_4 for sorption of CO_2 at moderate temperatures can be substantially enhanced by doping Li_4SiO_4 with alkali metals and other hetero-elements [21,22].

Green technology or the use of environment-friendly chemical processes is gaining attractiveness [23–25] because of the demand from conscientious consumers and strict environmental regulations. Hence, the use of rice husk ash (RHA), an undesirable agricultural mass residue, or fly ash (FA) from coal combustion in power plants as sources of silica for lithium silicate preparation could be an efficient eco-friendly route. In a very recent study [26], Olivares-Marín et al. synthesized Li_4SiO_4-based sorbents from FA that could maintain high CO_2 sorption capacities in 10 cycle processes. Compared with FA, RHA has higher amorphous SiO_2 content [23,27]. Moreover, RHA also contains some amounts of metals [28–30], which may generate high-performance Li_4SiO_4-based sorbents for CO_2 capture.

* Corresponding author. Fax: +86 27 87545526.
E-mail address: guoxin@mail.hust.edu.cn (X. Guo).

0304-3894/$ – see front matter © 2011 Elsevier B.V. All rights reserved.
doi:10.1016/j.jhazmat.2011.02.040

Table 1
RHA and RHA–Li_4SiO_4 chemical components (wt%).

Samples	K_2O	Na_2O	CaO	MgO	SiO_2	Al_2O_3
RHA1	2.53	0.16	1.52	0.56	94.71	0.52
RHA2	0.06	0.05	0.68	0.24	98.84	0.13
RHA1–Li_4SiO_4	1.17	0.06	1.53	0.52	96.15	0.57
RHA2–Li_4SiO_4	0.03	0.02	0.65	0.19	99.01	0.10

Taking into account the significant amorphous SiO_2 and metals content in RHA, Li_4SiO_4-based sorbents from RHA for CO_2 capture were developed in this study. Pure Li_4SiO_4 was also prepared for comparison purposes. These prepared sorbents were characterized using analytical techniques and evaluated their performance in multicycle CO_2 capture experiments. In addition, a double exponential model simulating CO_2 absorption based on the proposed sorption/desorption pathway is presented.

2. Experimental

2.1. Sorbents

Rice husk was taken from a local rice mill at Wuhan City, China. Based from a previous study on RHA [31], two treated RHA samples, named RHA1 and RHA2, were burnt in a batch furnace at about 600 °C for 4 h in air. Each RHA sample was grounded and sieved to produce less than 100 μm particles for further use. RHA1 and RHA2 have different husk pretreatment process before calcination. Husks from RHA1 were rinsed several times with distilled water, while husks from RHA2 were treated with acid. Acid-treated rice husk was prepared by immersing rice husks in 10% conc. (weight) HCl aqueous solution at 100 °C for 2 h and washed repeatedly with water until no acid is detected in the filtrate. Both treated rice husks were all dried at 80 °C overnight.

Li_4SiO_4-based sorbents from RHA were prepared by using the solid-state reaction of Li_2CO_3 (99.5%) with RHA in a Li:Si mixture with molar ratio of 4.1:1. A lithium excess was added to prevent the volatility of Li_2O under high temperature. The powders were all calcined at 800 °C for 4 h. Powders were denoted as RHA1–Li_4SiO_4 and RHA2–Li_4SiO_4. For comparison, pure lithium silicate (P–Li_4SiO_4) was also prepared following the same method described before, starting from Li_2CO_3 and SiO_2 (average size: 5 μm, 99.5%). A fraction of all synthesized sorbents with particle size less than 100 μm was collected for characterization.

2.2. Characterization methods

The chemical composition of rice husk ash and sorbents were determined using Rigaku RIX 3000 X-ray Fluorescence (XRF) spectrometer. The structural parameters of the sorbents were resolved by powder X-ray diffraction (XRD) using a Rigaku Rotaflex D/Max-C system with Cu-Kα radiation as the X-ray source. The accelerating voltage and the applied current were 35 kV and 30 mA, respectively. The particle size and morphology of the samples were observed with a scanning electron microscope (SEM) S-4800. Specific surface area, pore volume, and pore size distribution of the sorbents were measured by Micromeritics ASAP 2020 nitrogen (N_2) adsorption–desorption analyzer.

2.3. CO_2 absorption

CO_2 absorption was tested using a thermogravimetric analyzer (TGA, STA 409). About 10 mg of the sorbent was placed into the sample pan and heated from room temperature to 1000 °C at a heating rate of 10 °C/min in 100 vol.% CO_2 while CO_2 flow used the TGA experiments was 50 mL/min. The analysis was carried out to observe sorption/desorption properties of the sorbents dynamically. Furthermore, CO_2 absorption isotherms of the sorbents were measured in 100 vol.% CO_2 at 500, 550, 600, and 650 °C for 2.5 h. The samples were weighed in the end of the experiment with another precise balance to check the accuracy of the TGA experiments.

The twin fixed bed reactor system was used to study CO_2 capture behavior of the sorbents through 15 carbonation/calcination cycles. The twin fixed bed reactor system includes a carbonation reactor and a calcination reactor designed at atmospheric pressure. A sample boat containing the sorbent could be shifted between the two reactors and the flow of the reacting gas can be adjusted using a flow meter. The temperature was controlled by a computer, and variation in sample mass during the multiple cycles was monitored using a high delicate electronic balance with a weight range and accuracy of 0–110 g ± 0.5 mg. Additional details can be found in our previous research [32]. Samples were calcined at 800 °C in 100% N_2 and carbonated at 650 °C in 100% CO_2 while CO_2 flow used in the fix bed experiments was 1 L/min. Duration of carbonation and calcination were 15 min and 10 min, respectively.

3. Results and discussion

3.1. Characterization

3.1.1. Composition and structure of the staring materials

The composition and XRD profiles of the starting RHA samples are given in Table 1 and Fig. 1, respectively. RHA1 contained mainly SiO_2 with small amounts of trace elements, such as potassium, sodium, calcium, magnesium and aluminum. An acid treated process was used to remove the impurities from the husk. The trace element content, especially alkali metals (K_2O and Na_2O), sharply decreased in RHA2 and the amount of SiO_2 increased. Metal impurities, such as Na and K, have been shown to have a eutectic reaction with SiO_2 during combustion of rice husks and results in a drastic decrease of the melting point of SiO_2 [33]. Thus, RHA1 showed a lower percentage of minor constituents ($2\theta = 27^\circ$) as shown in Fig. 1. However, RHA2 only presented a broad peak appearing around

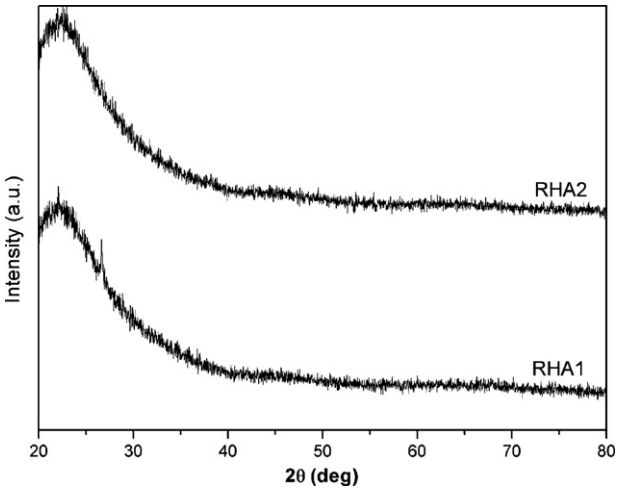

Fig. 1. XRD patterns of various pretreated RHA.

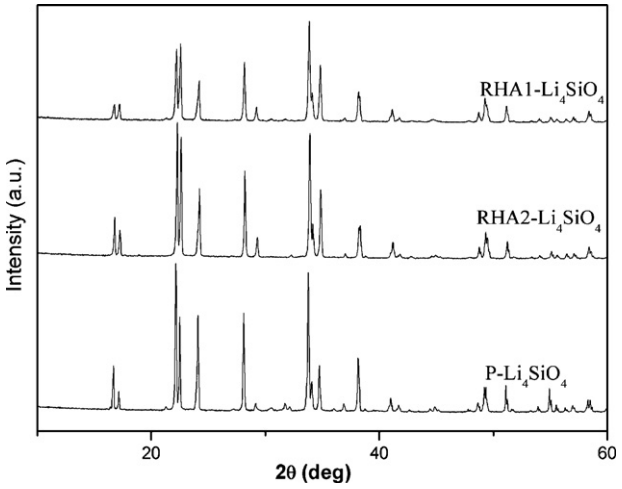

Fig. 2. XRD patterns of synthesized Li_4SiO_4-based sorbents.

($2\theta = 22^\circ$), which clearly indicates that RHA2 mainly consists of an amorphous silica [29] because alkali metals were removed from the husks during the acid-leaching treatment. XRD patterns of pure silica gel (99.5%) were similar to that of RHA2 (not shown here).

3.1.2. XRD results of prepared samples

After the Li_4SiO_4-based sorbent synthesis, samples were characterized by XRF and XRD. The metal impurities still existed in the Li_4SiO_4-based sorbents from RHA as presented in Table 1. However, the content decreased compared with RHA. Considering that some alkali metals sublimated at high temperature (>700 °C) [18], some alkali metals were lost during thermal treatments (800 °C). Fig. 2 shows the comparison of the XRD profiles of P–Li_4SiO_4 with those of the Li_4SiO_4-based sorbents from RHA. P–Li_4SiO_4 diffraction pattern fitted very well to JCPDS file 37-1472, which corresponds to the same compound. The presence of metal impurities in Li_4SiO_4-based sorbents from RHA did not modify the XRD patterns of the Li_4SiO_4 phase but produce a decrement on the XRD intensities. Veliz-Enriquez et al. [34] noted the expanded crystalline structures of doping Li_2ZrO_3 with alkali metals (K_2O and Na_2O) and the shift of the peaks. However, such results were not observed in the diffraction pattern of lithium-sodium orthosilicate ($Li_{4-x}Na_xSiO_4$). Veliz-Enriquez et al. suggested that lithium has a very small dispersion diffraction coefficient in comparison to the doping elements and the closed packed structure of the silicate. Therefore, the doping elements did not expect to diffuse so much into the Li_4SiO_4 network. Similar to $Li_{4-x}Na_xSiO_4$, the unchanged of the peaks observed here seemed to indicate that most of metal impurities were mainly located over the surface of Li_4SiO_4. Furthermore, a different phase (Li_3NaSiO_4) was observed in the study of Mejía-Trejo's. However, these similar phases, such as Li_3NaSiO_4 and Li_2KSiO_4, are not presented in this study. According to Mejía-Trejo's study, the solubility limit of sodium in Li_4SiO_4 is 0.1, $Li_{3.9}Na_{0.1}SiO_4$ [21]. In this study, the Na and K content were lower than the limit, resulting in lower quantities of Li_3NaSiO_4 and Li_2KSiO_4. Therefore, their abundance is beyond the XRD resolution.

3.1.3. Morphology of prepared samples

The Li_4SiO_4-based sorbents were characterized by SEM and surface morphologies of these sorbents are shown in Fig. 3. The grain size was measured using standard procedures. The P–Li_4SiO_4 showed dense polyhedral particles with particle size between 60 and 100 μm and formed agglomerates (Fig. 3a). This kind of morphology corresponds well with the high temperature used during the thermal treatment. Nevertheless, this morphology changed as a function of the metal impurities content. A slight increase in the metal content results in a change in the morphological characteristics of RHA2–Li_4SiO_4 (Fig. 3b). The particle size decreased to less than 45 μm and formed agglomerates. Moreover, as the metal

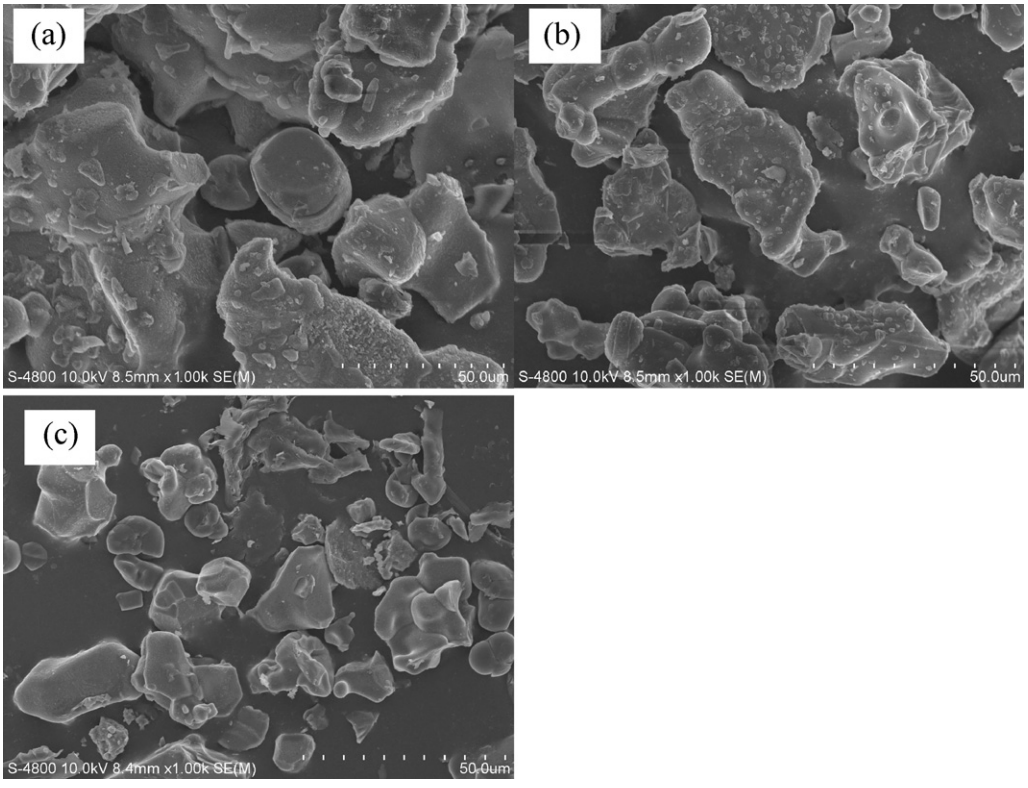

Fig. 3. SEM images of synthesized Li_4SiO_4-based sorbents.

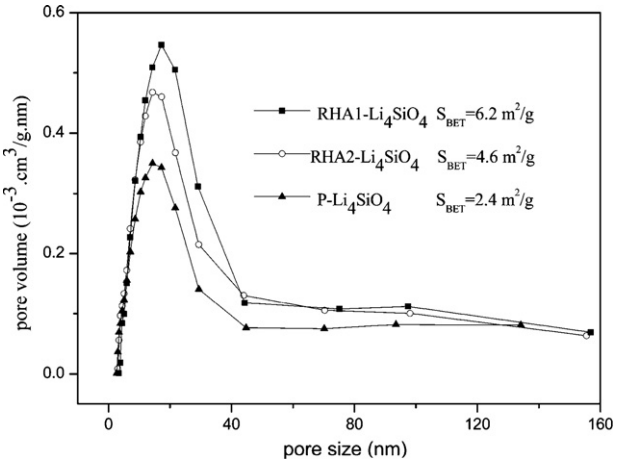

Fig. 4. Pore size distributions of synthesized Li_4SiO_4-based sorbents.

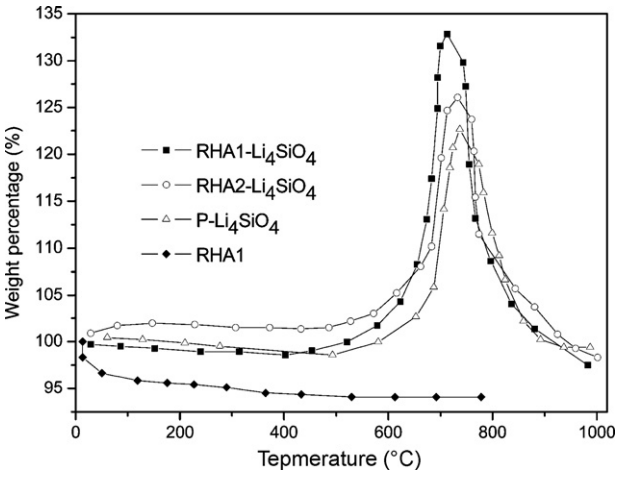

Fig. 5. Thermogravimetric analyses of synthesized Li_4SiO_4-based sorbents.

impurities content was further increased, RHA1–Li_4SiO_4 (Fig. 3c) showed a totally different morphology. The particles were not polyhedral corrugated and particle size decreased to 16 μm. The morphology of these samples is similar to doping lithium ceramics with alkali metals. It appeared that alkali metals inhibited the growing of the particles. Additionally, other elements, especially Mg [35] and Al [36] were reported to decrease the sintering effect of other oxides. The presence of these elements could resist the sintering effect of Li_2O, and thereby resulted in the smaller particles in Fig. 3.

3.1.4. BET results of prepared samples

SEM analysis revealed that the alkali metals (mainly K_2O) of RHA inhibited the growth of the particles, which may result to materials with more pores and higher surface area. To verify this hypothesis, N_2 adsorption analysis was performed. The pore size distributions of three Li_4SiO_4-based sorbents are plotted in Fig. 4. Only one peak, mainly located in the range of 0–20 nm, in each pore size distribution curve was observed. None of the samples presented a high surface area. However, pore volume and surface area showed an increasing trend as the metal impurities was added. RHA1–Li_4SiO_4 contains higher metal impurities content resulting to decreased particle size as seen in SEM analysis and sample exhibited larger surface area and larger pore volume. Conversely, P–Li_4SiO_4 has no metal impurities content resulting to bigger particles, lower surface area, and lower pore volume. Therefore, metal impurities in the Li_4SiO_4 system acted as a growth controller of the particles.

3.2. CO_2 sorption capacities

As was previously mentioned, Li_4SiO_4 is a promising CO_2 absorbent material. Moreover, enhancing CO_2 absorption on lithium ceramics by addition of potassium or sodium has been reported for other ceramics. If Li_4SiO_4-based RHA sorbents present a synergetic effect, these sorbents should capture CO_2 more efficiently than P–Li_4SiO_4 with a reaction represented as follows:

$$Li_{4-x}M_xSiO_4 + CO_2 \leftrightarrow Li_{2-x}M_{x/2}CO_3 + Li_{2-x}M_{x/2}SiO_3 \quad (2)$$

where M denotes potassium and sodium, $Li_{2-x}M_{x/2}CO_3$ represents only a mixture of Li_2CO_3, K_2CO_3 and Na_2CO_3.

The RHA samples contain CaO; however, this CaO may be inactive with regard to its use in CO_2 capture, but this hypothesis was also verified by subjecting the RHA samples to CO_2 sorption process. Due to RHA1 sample containing high contents of CaO, typical results are given in Fig. 5 for RHA1. It can be seen that mass increase of the RHA1 during the carbonation stage was negligible, which confirmed a negligible contribution to the capture from these element of Ca.

Fig. 5 also shows the thermograms of these Li_4SiO_4 sorbents in 100% CO_2 and presents a qualitative scheme of CO_2 absorption behavior. P–Li_4SiO_4 gave a standard CO_2 absorption, as was previously reported [18]. The sample began to absorb CO_2 at around 450 °C, finishing this process at 710 °C with 22.1 wt% maximum absorption. At temperature higher than 710 °C, the sample presented a desorption process. Due to lower potassium and sodium content, the CO_2 sorption capacities of RHA2–Li_4SiO_4 only showed a little improvement in comparison with the P–Li_4SiO_4. However, RHA1–Li_4SiO_4, which has the highest potassium and sodium content, showed a significantly improved CO_2 absorption, increasing to 10.3 wt% and a total CO_2 absorption of 32.4 wt%. Furthermore, the absorption seemed to be faster in RHA1–Li_4SiO_4 in comparison with the first two samples due to the higher slope observed on the sorption temperature range. The same behavior was observed using pure Li_4SiO_4 and sodium orthosilicates. These results confirm that CO_2 absorption reactivity is enhanced by metal impurities in the samples. P–Li_4SiO_4 and RHA1–Li_4SiO_4 were analyzed in the further study.

3.3. Kinetic analysis of CO_2 absorption

A double exponential model was successfully used to simulate the CO_2 absorption on lithium-based sorbents such as Li_4SiO_4 [18], $Li_{4-x}Na_xSiO_4$ [21], and Li_5AlO_4 [14]. This model can be represented as:

$$y = A \exp -k_1 t + B \exp -k_2 t + C \quad (3)$$

where y represents the weight change of CO_2 absorbent, t is the time, k_1 and k_2 are the rate constants for the CO_2 chemisorption produced directly over the Li_4SiO_4 particles and CO_2 chemisorption kinetically controlled by lithium diffusion [37,38], respectively. In addition, the pre-exponential factors A and B indicate the intervals at which each process controls the whole CO_2 capture process, and the C constant indicates the y-intercept. Initially, CO_2 reacts with the Li_2O component of Li_4SiO_4 and produces a Li_2CO_3 external shield. Subsequently, when the external layer is completely formed, the lithium diffuses across the carbonate layer in order to reach the surface and react with CO_2 (diffusion process).

P–Li_4SiO_4 and RHA1–Li_4SiO_4 isotherms are shown in Figs. 6 and 7, respectively. Fig. 6 presents the isothermal graphs of P–Li_4SiO_4 at different temperatures. Qualitatively, CO_2 absorption increased as a function of the temperature as expected. After 2.5 h at 500 °C, the ceramic absorbed only 3.8 wt%. At 650 °C, the

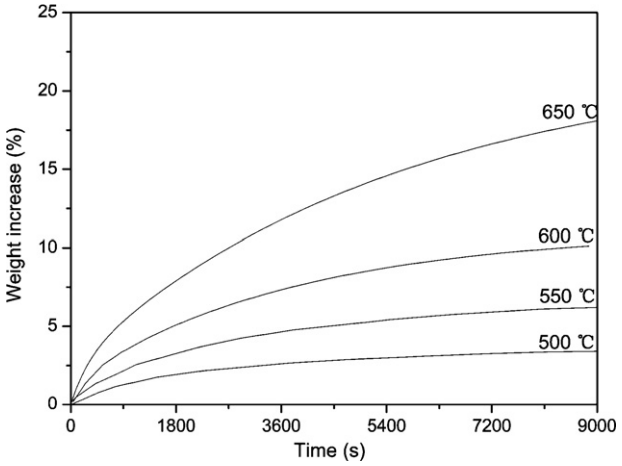

Fig. 6. Isotherms of the CO_2 sorption on the P–Li_4SiO_4 sample.

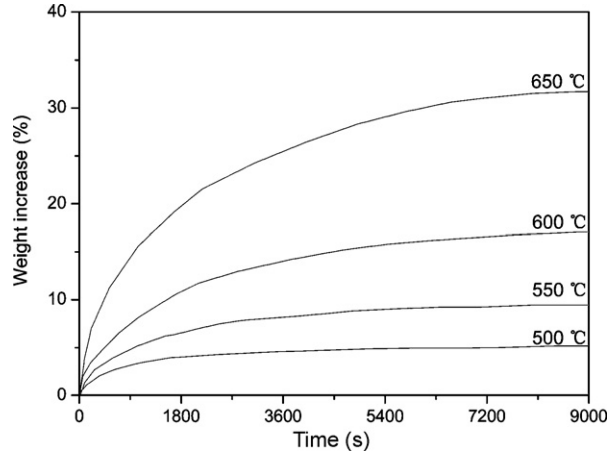

Fig. 7. Isotherms of the CO_2 sorption on the RHA1–Li_4SiO_4 sample.

Table 2
Kinetic parameters obtained from the isotherms of P–Li_4SiO_4.

T (°C)	k_1 (s)	k_2 (s)	R
500	7.13×10^{-4}	4.73×10^{-5}	0.9997
550	1.26×10^{-3}	1.14×10^{-4}	0.9997
600	2.21×10^{-3}	1.81×10^{-4}	0.9999
650	4.40×10^{-3}	4.23×10^{-4}	0.9996

absorption increased to 18 wt% in the same period of time. The exponential constant values obtained at each temperature are presented in Table 2. k_1 values are at least 1 order of magnitude higher than those of k_2, revealing that the lithium diffusion is the limiting step in the absorption process. These results are in agreement with previous reports [18,21].

A similar, but more drastic, behavior was observed on the isotherms of the RHA1–Li_4SiO_4 (Fig. 7). The kinetic constant values (Table 3) were higher than those obtained for the P–Li_4SiO_4 sample. Both chemisorption and diffusion constant values were enhanced

Table 3
Kinetic parameters obtained from the isotherms of RHA1–Li_4SiO_4.

T (°C)	k_1 (s)	k_2 (s)	R
500	2.40×10^{-3}	1.22×10^{-4}	0.9990
550	3.35×10^{-3}	1.92×10^{-4}	0.9996
600	4.85×10^{-3}	2.66×10^{-4}	0.9995
650	7.76×10^{-3}	6.03×10^{-4}	0.9995

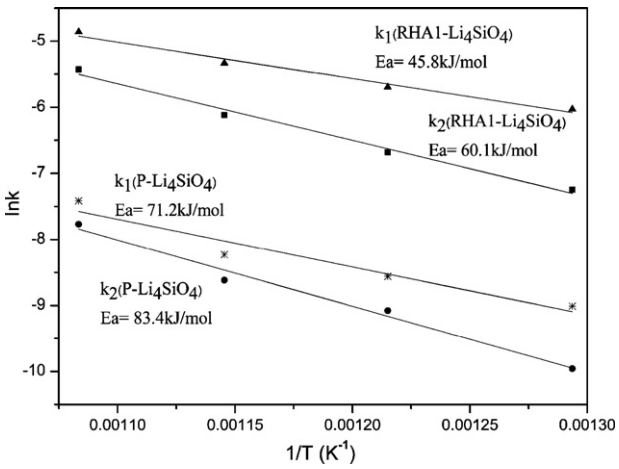

Fig. 8. Plots of $\ln k$ versus $1/T$ for the two different processes of chemisorption (k_1) and diffusion (k_2) on P–Li_4SiO_4 and RHA1–Li_4SiO_4.

by potassium and sodium addition, which is in agreement with previous reports on pure Li_4SiO_4 and sodium orthosilicates [21].

Furthermore, Fig. 8 shows the well-fitted linear trends for the plots of $\ln k$ versus $1/T$. If the kinetic constant values (i.e., k_1 or k_2) are linear-dependent with the corresponding temperatures ($1/T$), the gradients of these best-fit lines may follow an Arrhenius-type behavior, which can be written as:

$$K = k_0 \exp^{(-Ea/RT)} \quad (4)$$

in which k_0 is the reaction rate constant, E_a is the activation energy of the chemisorption process and diffusion process, R is the gas constant, and T is the absolute temperature. Consequently, the activation energies for the chemisorption processes and diffusion processes in P–Li_4SiO_4 can be estimated to be 71.2 and 83.4 kJ/mol, respectively. This further confirms that lithium diffusion is the limiting step in the whole absorption process. Moreover, compared with P–Li_4SiO_4, the activation energy of RHA1–Li_4SiO_4 obtained for both processes decreased. A similar behavior was also observed in pure Li_4SiO_4 and potassium-doped Li_4SiO_4-based sorbents from FA [26]. Venegas et al. examined the particle size effect on the CO_2 sorption process and found that lithium, on the small particles, does not have to diffuse at such long distances as on the large particles [18]. Consequently, the lithium diffusion activation energies of the small particles were smaller than those obtained for the large particles. In this study, the presence of higher metals resulted in

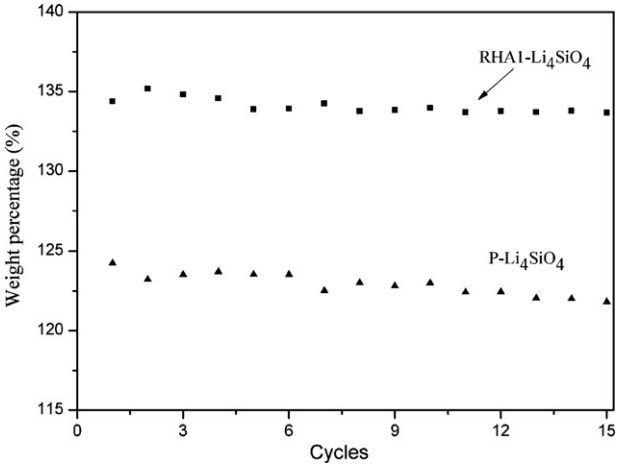

Fig. 9. Multiple cycles of CO_2 sorption (15 min) and desorption (10 min) on P–Li_4SiO_4 and RHA1–Li_4SiO_4 under the same experimental conditions.

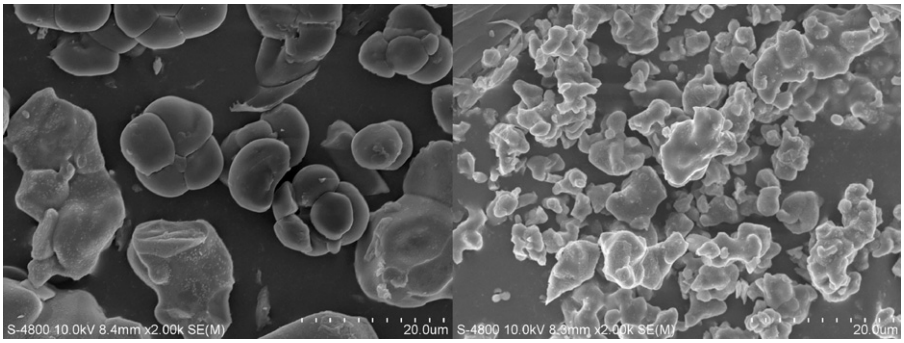

Fig. 10. SEM images of synthesized RHA1–Li_4SiO_4 sorbent and the sorbent after 15 sorption/desorption cycles.

formation of smaller particles, as seen in SEM analysis. The smaller particles of RHA1–Li_4SiO_4 can decrease the activation energy of the diffusion process. On the other hand, Venegas et al. [18] suggested that larger pore volume and surface area of RHA1–Li_4SiO_4 was associated with the presence of more lithium atoms over the surface of the particles. RHA1–Li_4SiO_4, exhibiting larger surface area and larger pore volume (observed in BET results), can thus decrease activation energy in the chemisorption process. As a consequence of these double effects, CO_2 absorption reactivity is improved significantly in RHA1–Li_4SiO_4.

3.4. Multicycle properties

For a continuous process to be feasible, the material must operate over numerous sorption/desorption cycles. The working cyclic capacity, stability, and lifetime of the sorbents can be determined using this method. Initially, P–Li_4SiO_4 and RHA1–Li_4SiO_4 were investigated by carrying out 15 CO_2 sorption/desorption cycles and results are presented in Fig. 9. As expected, the absorption amount in both samples remained almost unchanged even after 15 cycles. Moreover, RHA1–Li_4SiO_4 maintained higher CO_2 within the defined absorption time, indicating that this sorbent may be a new option for CO_2 absorption.

Higher potassium and sodium content could cause sintering during the sorption/desorption processes, which may slow down the CO_2 diffusion and subsequently reduce the absorption capacity within the defined absorption time. To further understand the effect of potassium and sodium addition, the morphology of RHA1–Li_4SiO_4 before and after 15 cycles were analyzed as shown in Fig. 10. Compared with the SEM image of the initial sorbent, the surface of calcined sample appears loose and porous, and CO_2 may diffuse easily into the interior of the sorbent during the sorption process, which shows the good regenerability properties of RHA1–Li_4SiO_4.

4. Conclusions

The Li_4SiO_4-based sorbents derived from RHA for CO_2 absorption at high temperatures were developed. XRD results showed that metals of RHA were doped with Li_4SiO_4 resulting to inhibited particle growth and increased pore volume and surface area as proven by SEM and N_2 adsorption. The presence of metals in the Li_4SiO_4-based sorbent produced an increase in the kinetic reaction of the CO_2 sorption when compared with pure Li_4SiO_4. Isothermal analyses further indicated that the sorbents adjust to the same CO_2 sorption mechanism: a chemical sorption process followed by a lithium diffusion process. However, the activation energies of the Li_4SiO_4-based sorbent prepared from RHA1 were smaller than that of pure Li_4SiO_4. These results were explained in terms of reactivity for the chemisorption process and in terms of geometry for the diffusion process. Moreover, the sorbent can maintain the higher absorption capacities during multiple sorption/desorption cycles, showing that this sorbent may be a new option for CO_2 absorption at high temperature.

Acknowledgements

This work was supported by the National Natural Science Foundation of China (grant no. 50936001,51021065) and the National Key Basic Research and Development Program of China (grant no. 2011CB201500, 2011CB707301).

References

[1] A.W.C. van den Berg, C.O. Arean, Materials for hydrogen storage: current research trends and perspectives, Chem. Commun. (2008) 668–681.
[2] H. Yang, Z. Xu, M. Fan, R. Gupta, R.B. Slimane, A.E. Bland, I. Wright, Progress in carbon dioxide separation and capture: a review, J. Environ. Sci. 20 (2008) 14–27.
[3] J. Blamey, E.J. Anthony, J. Wang, P.S. Fennell, The calcium looping cycle for large-scale CO_2 capture, Prog. Energy Combust. Sci. 36 (2010) 260–279.
[4] M.Z. Jacobson, Review of solutions to global warming, air pollution, and energy security, Energy Environ. Sci. 2 (2009) 148–173.
[5] L.M. Romeo, Y. Lara, P. Lisbona, A. Martinez, Economical assessment of competitive enhanced limestones for CO_2 capture cycles in power plants, Fuel Process. Technol. 90 (2009) 803–811.
[6] E. Ochoa-Fernández, M. Rønning, T. Grande, D. Chen, Synthesis and CO_2 capture properties of nanocrystalline lithium zirconate, Chem. Mater. 18 (2006) 6037–6046.
[7] J.i. Ida, Y.S. Lin, Mechanism of high-temperature CO_2 sorption on lithium zirconate, Environ. Sci. Technol. 37 (2003) 1999–2004.
[8] R.B. Khomane, B.K. Sharma, S. Saha, B.D. Kulkarni, Reverse microemulsion mediated sol-gel synthesis of lithium silicate nanoparticles under ambient conditions: scope for CO_2 sequestration, Chem. Eng. Sci. 61 (2006) 3415–3418.
[9] H. Pfeiffer, E. Lima, P. Bosch, Lithium-sodium metazirconate solid solutions, $Li_{2-x}Na_xZrO_3$ ($0 \le x \le 2$): a hierarchical architecture, Chem. Mater. 18 (2006) 2642–2647.
[10] T. Zhao, E. Ochoa-Fernández, M. Rønning, D. Chen, Preparation and high-temperature CO_2 capture properties of nanocrystalline Na_2ZrO_3, Chem. Mater. 19 (2007) 3294–3301.
[11] M. Kato, Kazuaki Nakagawa, Kenji Essaki, Yukishige Maezawa, Shin Takeda, Ryosuke Kogo, Y. Hagiwara, Novel CO_2 absorbents using lithium-containing oxide, Int. J. Appl. Ceram. Technol. 2 (2005) 467–475.
[12] B.N. Nair, R.P. Burwood, V.J. Goh, K. Nakagawa, T. Yamaguchi, Lithium based ceramic materials and membranes for high temperature CO_2 separation, Prog. Mater. Sci. 54 (2009) 511–541.
[13] L.M. Palacios-Romero, E. Lima, H. Pfeiffer, Structural analysis and CO_2 chemisorption study on nonstoichiometric lithium cuprates ($Li_{2+x}CuO_{2+x/2}$), J. Phys. Chem. A 113 (2008) 193–198.
[14] T. Ávalos-Rendón, J. Casa-Madrid, H. Pfeiffer, Thermochemical capture of carbon dioxide on lithium aluminates ($LiAlO_2$ and Li_5AlO_4): a new option for the CO_2 absorption, J. Phys. Chem. A 113 (2009) 6919–6923.
[15] R. Xiong, J. Ida, Y.S. Lin, Kinetics of carbon dioxide sorption on potassium-doped lithium zirconate, Chem. Eng. Sci. 58 (2003) 4377–4385.
[16] S. Kimura, M. Adachi, R. Noda, M. Horio, Particle design and evaluation of dry CO_2 recovery sorbent with a liquid holding capability, Chem. Eng. Sci. 60 (2005) 4061–4071.
[17] K. Essaki, M. Kato, Influence of temperature and CO_2 concentration on the CO_2 absorption properties of lithium silicate pellets, J. Mater. Sci. 40 (2005) 5017–5019.

[18] M.J. Venegas, E. Fregoso-Israel, R. Escamilla, H. Pfeiffer, Kinetic and reaction mechanism of CO_2 sorption on Li_4SiO_4: study of the particle size effect, Ind. Eng. Chem. Res. 46 (2007) 2407–2412.
[19] M.E. Bretado, V.G. Velderrain, D.L. Gutiérrez, V. Collins-Martínez, A.L. Ortiz, A new synthesis route to Li_4SiO_4 as CO_2 catalytic/sorbent, Catal. Today 107–108 (2005) 863–867.
[20] X. Wu, Z. Wen, X. Xu, X. Wang, J. Lin, Synthesis and characterization of Li_4SiO_4 nano-powders by a water-based sol-gel process, J. Nucl. Mater. 392 (2009) 471–475.
[21] V.L. Mejía-Trejo, E. Fregoso-Israel, H. Pfeiffer, Textural, structural, and CO_2 chemisorption effects produced on the lithium orthosilicate by its doping with sodium ($Li_{4-x}Na_xSiO_4$), Chem. Mater. 20 (2008) 7171–7176.
[22] C. Gauer, W. Heschel, Doped lithium orthosilicate for absorption of carbon dioxide, J. Mater. Sci. 41 (2006) 2405–2409.
[23] L.C. Lau, K.T. Lee, A.R. Mohamed, Rice husk ash sorbent doped with copper for simultaneous removal of SO_2 and NO: optimization study, J. Hazard. Mater. 183 (2010) 738–745.
[24] M. Bhagiyalakshmi, L.J. Yun, R. Anuradha, H.T. Jang, Utilization of rice husk ash as silica source for the synthesis of mesoporous silicas and their application to CO_2 adsorption through TREN/TEPA grafting, J. Hazard. Mater. 175 (2010) 928–938.
[25] Y. Li, C. Zhao, Q. Ren, L. Duan, H. Chen, X. Chen, Effect of rice husk ash addition on CO_2 capture behavior of calcium-based sorbent during calcium looping cycle, Fuel Process. Technol. 90 (2009) 825–834.
[26] M. Olivares-Marín, T.C. Drage, Maroto-Valer, M. Mercedes, Novel lithium-based sorbents from fly ashes for CO_2 capture at high temperatures, Int. J. Greenhouse Gas Control 4 (2010) 623–629.
[27] I. Dahlan, Z. Ahmad, M. Fadly, K.T. Lee, A.H. Kamaruddin, A.R. Mohamed, Parameters optimization of rice husk ash (RHA)/CaO/CeO_2 sorbent for predicting SO_2/NO sorption capacity using response surface and neural network models, J. Hazard. Mater. 178 (2010) 249–257.
[28] V.C. Srivastava, I.D. Mall, I.M. Mishra, Equilibrium modeling of ternary adsorption of metal ions onto rice husk ash, J. Chem. Eng. Data 54 (2009) 705–711.
[29] Q. Feng, Q. Lin, F. Gong, S. Sugita, M. Shoya, Adsorption of lead and mercury by rice husk ash, J. Colloid Interface Sci. 278 (2004) 1–8.
[30] R.V. Krishnarao, J. Subrahmanyam, T. Jagadish Kumar, Studies on the formation of black particles in rice husk silica ash, J. Eur. Ceram. Soc. 21 (2001) 99–104.
[31] T.H. Liou, S.J. Wu, Kinetics study and characteristics of silica nanoparticles produced from biomass-based material, Ind. Eng. Chem. Res. 49 (2010) 8379–8387.
[32] K. Wang, X. Guo, P. Zhao, C. Zheng, Cyclic CO_2 capture of CaO-based sorbent in the presence of metakaolin and aluminum (hydr)oxides, Appl. Clay Sci. 50 (2010) 41–46.
[33] J. Umeda, K. Kondoh, High-purification of amorphous silica originated from rice husks by combination of polysaccharide hydrolysis and metallic impurities removal, Ind. Crops Prod. 32 (2010) 539–544.
[34] M.Y. Veliz-Enriquez, G. Gonzalez, H. Pfeiffer, Synthesis and CO_2 capture evaluation of $Li_{2-x}K_xZrO_3$ solid solutions and crystal structure of a new lithium-potassium zirconate phase, J. Solid State Chem. 180 (2007) 2485–2492.
[35] W. Liu, B. Feng, Y. Wu, G. Wang, J. Barry, J.C. Diniz da Costa, Synthesis of sintering-resistant sorbents for CO_2 capture, Environ. Sci. Technol. 44 (2010) 3093–3097.
[36] B.M. Steenari, O. Lindqvist, High-temperature reactions of straw ash and the anti-sintering additives kaolin and dolomite, Biomass Bioenergy 14 (1998) 67–76.
[37] R. Rodríguez-Mosqueda, H. Pfeiffer, Thermokinetic analysis of the CO_2 chemisorption on Li_4SiO_4 by using different gas glow rates and particle sizes, J. Phys. Chem. A 114 (2010) 4535–4541.
[38] L. Martínez-dlCruz, H. Pfeiffer, Effect of oxygen addition on the thermokinetic properties of CO_2 chemisorption on Li_2ZrO_3, Ind. Eng. Chem. Res. 49 (2010) 9038–9042.